Available online at www.sciencedirect.com
ScienceDirect
Bioorganic & Medicinal Chemistry Letters 18 (2008) 1869–1873
Bioorganic & Medicinal Chemistry Letters

Potent antagonists of the CCR2b receptor. Part 3: SAR of the (*R*)-3-aminopyrrolidine series

Wilna J. Moree,[a,*] Ken-ichiro Kataoka,[b] Michele M. Ramirez-Weinhouse,[a,†] Tatsuki Shiota,[b] Minoru Imai,[b] Takaharu Tsutsumi,[b] Masaki Sudo,[b,‡] Noriaki Endo,[b] Yumiko Muroga,[b] Takahiko Hada,[b,§] Dewey Fanning,[a,¶] John Saunders,[a,¶] Yoshinori Kato,[b] Peter L. Myers[a,††] and Christine M. Tarby[a,‡‡]

[a]*Deltagen Research Laboratories (Former CombiChem, Inc.), 4570 Executive Drive, San Diego, CA 92121, USA*
[b]*Teijin Institute for Biomedical Research, 4-3-2 Asahigaoka, Hino, Tokyo, 191-8512, Japan*

Received 21 December 2007; revised 4 February 2008; accepted 7 February 2008
Available online 10 February 2008

Abstract—SAR studies were conducted around lead compound **1** using high-throughput parallel solution and solid phase synthesis. Our lead optimization efforts led to the identification of several CCR2b antagonists with potent activity in both binding and functional assays [Compound **71** CCR2b Binding IC_{50} 3.2 nM; MCP-1-Induced Chemotaxis IC_{50} 0.83 nM; Ca^{2+} Flux IC_{50} 7.5 nM].

Chemokines or chemotactic cytokines are small molecular weight (6–15 kD) proteins that modulate inflammatory and immune responses through promotion of cell migration, cell adhesion and transmigration.[1] They are divided into four classes dependent on the arrangement of conserved cysteines in the N-terminal region. Monocyte Chemoattractant Protein-1 (MCP-1) is a member of the CC-chemokine family and selectively recruits leukocytes from the circulation to the site of inflammation through binding with the CCR2b receptor.[2] This receptor is a member of the seven transmembrane receptor family (7-TM) and is expressed on the surface of monocytes and macrophages.

Studies with CCR2[3] and MCP-1[4] knock-out mice have indicated that antagonists of the CCR2b receptor may exert therapeutic effects in a variety of inflammatory diseases including rheumatoid arthritis,[5] atherosclerosis,[6] glomuleronephritis,[7] and multiple sclerosis.[8] This prompted our laboratories and others,[9] to develop small molecular weight inhibitors of the interaction between MCP-1 and the CCR2b receptor.

In our previous manuscripts,[10] we described the discovery of several diamine based lead compounds as CCR2b antagonists. Compound **1**, containing a (*R*)-3-aminopyrrolidine core, was identified as a key lead structure with good activity in a [^{125}I]-MCP-1 binding assay (IC_{50} 180 nM) and in a CCR2b-mediated chemotaxis assay (IC_{50} 24 nM). Herein we report our structure activity relationship (SAR) studies around this lead compound with the objective of generating potent and selective CCR2b antagonists.

Three fragments were defined for optimization as illustrated in Figure 1; the R^1 substituted *N*-benzyl group, the amino acid, and the R^2 substituted benzamide. In order to conduct the lead optimization studies in the (*R*)-3-aminopyrrolidine series, both solution and solid-phase methodologies were developed. Using solution

Keywords: CCR2b; Chemokine; Antagonist.
* Corresponding author at present address: Neurocrine Biosciences, 12790 El Camino Real, San Diego, CA 92130, USA. Tel.: +1 858 617 7506; fax: +1 858 617 7925; e-mail: wmoree@neurocrine.com
† Present address: Pfizer Global Research & Development, La Jolla Laboratories, Discovery Chemistry, 10614 Science Center Drive (CB6), San Diego, CA 92121, USA.
‡ Present address: Pfizer Global Research and Development, Nagoya Laboratories, 5-2 Taketoyo, Aichi 470-2393, Japan.
§ Present address: Bizen Chemical Co., Ltd, Research and Development Department, 363-Tokutomi, Kumayama-Cho, Akaiwa-Gun, Okayama 709-0716, Japan.
¶ Present address: Vertex, 11010 Torreyana Road, San Diego, CA 92121, USA.
†† Present address: LEAD Therapeutics, Inc., 999 Bayhill Drive, Suite 130, San Bruno, CA 94066, USA.
‡‡ Present address: Bristol-Myers Squibb Company, PO Box 4000, Princeton, NJ 08543, USA.

0960-894X/$ - see front matter © 2008 Elsevier Ltd. All rights reserved.
doi:10.1016/j.bmcl.2008.02.015

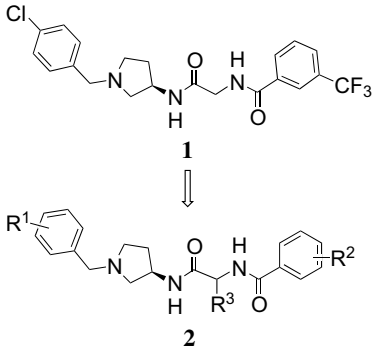

Figure 1. Lead optimization plan for Compound **1**.

synthesis, the R^1 substituted *N*-benzyl group was examined independently of the amino acid and R^2 substituted benzamide (Scheme 1). (*R*)-1-Benzyl-3-aminopyrrolidine **3** was converted to **4** through the following sequence: EDCI-mediated coupling with *N*-Boc-glycine, removal of the *N*-Boc-protecting group, acylation with *m*-trifluoromethyl benzoyl chloride, and debenzylation by hydrogenolysis. High-throughput alkylation or reductive amination chemistry afforded the desired compounds **5**, which were purified using acid–base extraction.

The amino acid portion of the molecule and the R^2 substituted benzamide were examined in concert, while maintaining the 4-chlorobenzyl substitution on the pyrrolidine nitrogen (Scheme 2). (*R*)-3-*N*-Boc-pyrrolidine **6** was alkylated with *p*-chlorobenzyl chloride, followed by the TFA deprotection of *N*-Boc group. A variety of commercially available *N*-Boc-protected natural and unnatural amino acids were used and coupled to the 3-amino group of the pyrrolidine. Following *N*-deprotection, the resulting intermediates **7** were coupled in a high-throughput fashion to a variety of acids. The coupling conditions employed allowed for extractive purification of the final product. These products were typically produced in >90% purity as determined by HPLC.

In order to effectively vary the R^1 substituted *N*-benzyl group and the R^2 substituted benzamide, simultaneously, a solid phase synthesis route was devised (Scheme 3). Fmoc-protected (*R*)-3-aminopyrrolidine preloaded with an amino acid of interest (**9**) was intro-

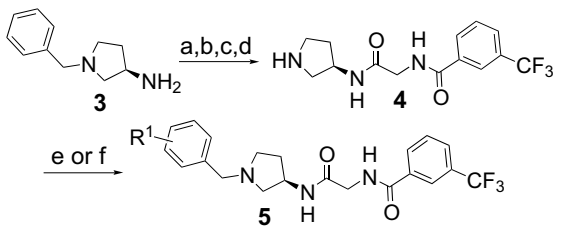

Scheme 1. Reagents and conditions: (a) *N*-Boc-Glycine, EDCI, HOBt, TEA; (b) 3 M HCl-CH_3OH; (c) *m*-CF_3-PhCOCl, TEA; (d) H_2, $Pd(OH)_2$-C, MeOH; (e) R^1PhCH_2Cl or R^1PhCH_2Br, (piperidinomethyl)polystyrene, CH_3CN, 50°C; (f) R^1PhCHO, $NaBH_3CN$, 2.5% aq, AcOH, MeOH, 60 °C.

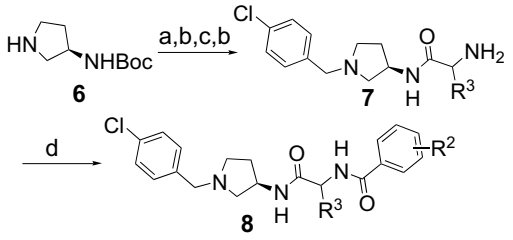

Scheme 2. Reagents: (a) *p*-chlorobenzyl chloride, K_2CO_3; (b) TFA; (c) *N*-Boc-CH(R^3)-CO_2H, EDCI, HOBt, $^iPr_2NEt$; (d) R^2PhCO_2H, EDCI, HOBt, $^iPr_2NEt$.

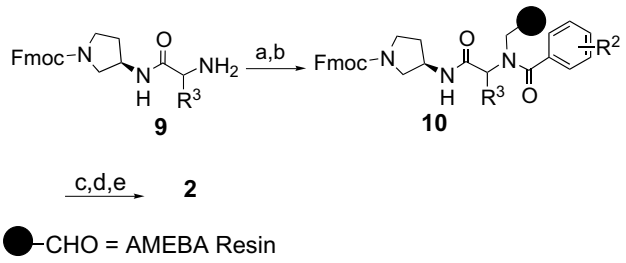

Scheme 3. Reagents and conditions: (a) AMEBA resin, $NaBH(OAc)_3$, 1% HOAc-DMF; (b) R^2PhCO_2H, HBTU, $^iPr_2NEt$, DMF, 1 h; (c) 20% piperidine-DMF, 10 min; (d) R^1PhCHO, $NaBH(OAc)_3$, 1% HOAc-DMA; (e) 95% TFA.

duced onto acid sensitive methoxybenzaldehyde (AMEBA) resin[11] by reductive amination. Coupling with a variety of benzoic acids provided **10**. Following removal of the Fmoc-protecting group, reductive amination with aromatic aldehydes provided the fully functionalized final products, which were cleaved from resin with TFA and purified using ion exchange chromatography. The purities of all compounds synthesized by solid and solution phase chemistries were assessed by HPLC and compounds were re-purified via mass-triggered reverse phase HPLC[12] if found to be less than 85% pure.

The compounds were evaluated in a radioligand binding assay using [^{125}I]-MCP-1 and THP-1 cells.[13] Potent compounds were then subsequently tested in a MCP-1-induced cell chemotaxis assay using THP-1 as the chemotactic cell line.[14] The results for selected compounds are summarized in Tables 1–3.

We first sought to optimize the R^1 substituted benzyl group (Table 1). An initial set of compounds (**1**, **12**–**20**), was prepared based on the Topliss optimization tree.[15] The resulting SAR indicated a clear preference for *p*-substitution on the benzyl ring. The *p*-substituted compounds (**1**, **19**–**20**) were 4- to 8-fold more potent than **12** (R = H) and the *o*-substituted variants (**13**–**15**) and at least 25-fold more potent than *m*-substituted compounds (**16**–**18**). Based on this observation, the range of substituents at the 4-position of the benzyl ring was expanded. Small electron donating groups (**19**–**23**) were preferred over electron withdrawing substituents (**28**–**30**). Additionally 2,4- and 3,4-substitution patterns were tolerated and either maintained or slightly improved activity (**31**–**33**). The functional activities of

Table 1. Binding affinity to CCR2b and CCR2-mediated chemotaxis activity for (*R*)-3-amino-pyrrolidine series

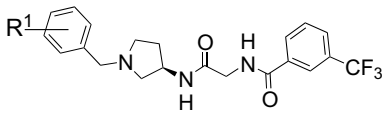

Compound	R^1	Binding IC_{50}[a] (nM)	Chemotaxis IC_{50}[a] (nM)
12	H	690	418
13	2-Cl	630	418
14	2-CH_3	960	127
15	2-OCH_3	1360	nd[b]
16	3-Cl	>5000	nd
17	3-CH_3	3100	nd
18	3-OCH_3	3170	nd
1	4-Cl	180	24
19	4-CH_3	116 (31)	12.4 (0.3)
20	4-OCH_3	114	35
21	4-Et	59	9.4
22	4-Br	166	21
23	4-Vinyl	121	6.2
24	4-CH_3S	204 (108)	21
25	4-OH	226	5.5
26	4-NHAc	305	nd
27	4-OCF_3	610	103
28	4-F	960	121
29	4-NO_2	1550	nd
30	4-CN	2650	nd
31	2,4-$(CH_3)_2$	54	16
32	2,4-Cl_2	300 (223)	286
33	4-OH, 3-OCH_3	153	77
34	2-Naphthyl	759	74

[a] IC_{50} values were derived from dose response curves generated from duplicate data points. Values with standard deviations (in parentheses) are means of at least three independent experiments.
[b] nd = not determined.

the compounds, assessed in a chemotaxis assay, demonstrated a loose correlation with the binding data.

We next examined a variety of R^3 amino acid spacers simultaneously with replacements for the R^2 substituted benzamide functionality. Although many different α and ß-amino acids were screened, only the glycine spacer consistently afforded compounds with an appropriate level of CCR2 binding activity for further optimization.[16] Likewise the incorporation of aliphatic amides instead of R^2 substituted benzamides completely abolished CCR2 activity and will not be discussed further in this manuscript. Systematic optimization of the substituents on the benzamide ring (R^2) indicating meta-substitution on the aromatic ring was favored as exemplified by the comparison of compound **1**, **39** and **40** with **35**–**38** and **41**–**43** (Table 2). Using a Craig plot guided optimization,[17] we observed a preference for substituents with positive Hammett σ/Hansch π constants. This is illustrated by the comparison of active compounds **1** (CF_3), **46** (Br), **47** (OCF_3) and **50** (NO_2) with the inactive **44** (CN), **48**(NH_2), and **49** (OCH_3). The parent trifluoromethyl group was the most active single substituent identified for the ring. Further improvements in activity required incorporation of an additional functionality on this ring. Introduction of an aniline

Table 2. Variation of R^2 in (*R*)-3-aminopyrrolidine series

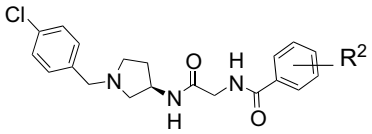

Compound	R^2	Binding IC_{50}[a] (nM)	Chemotaxis IC_{50}[a] (nM)
35	H	>10000	nd[b]
36	2-CH_3	>10000	nd
37	2-Cl	>10000	nd
38	2-CF_3	>10000	nd
39	3-CH_3	2380	nd
40	3-Cl	2400	nd
1	3-CF_3	180	24
41	4-CH_3	10000	nd
42	4-Cl	>5000	nd
43	4-CF_3	>5000	nd
44	3-CN	>10000	nd
45	3-F	4330	nd
46	3-Br	785	473 (163)
47	3-OCF_3	489	360
48	3-NH_2	>10000	nd
49	3-OCH_3	>10000	nd
50	3-NO_2	832	445
51	2-NH_2	>10000	nd
52	2-NH_2, 5-NO_2	208	43
53	2-NH_2, 5-Cl	730	nd
54	2-NH_2, 5-Br	643	nd
55	2-NH_2, 5-I	308	22
56	2-NH_2, 5-OCF_3	88	43
57	2-NH_2, 5-CF_3	26	3.6

[a] IC_{50} values were derived from dose response curves generated from duplicate data points. Values with standard deviations (in parentheses) are means of at least three independent experiments.
[b] nd = not determined.

Table 3. Binding affinity to CCR2b and CCR2-mediated chemotaxis activity for (*R*)-3-amino-pyrrolidine series

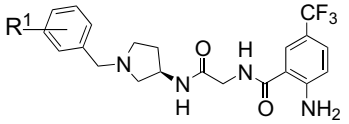

Compound	R^1 (substituted phenyl)	Binding IC_{50}[a] (nM)	Chemotaxis IC_{50}[a] (nM)
58	4-Cl	26	3.6
59	4-Br	116	2.6
60	4-CH_3	20	3.1
61	4-Et	11 (6)	0.89
62	4-Vinyl	19	3.9
63	4-OCH_3	20	11
64	4-OH	42	5.1
65	4-Cl, 3-NH_2	4.1	11
66	4-CH_3, 3-NH_2	6.1	12
67	4-OCH_3, 3-NH_2	5.3	8.8
68	4-OH, 3-NH_2	14	18
69	4-OCH_3, 3-OH	53	9.2
70	4-OH, 3-OCH_3	39	14
71	2,4-$(CH_3)_2$	3.2 (2.6)	0.83
72	2,4-Cl_2	96	nd[b]

[a] IC_{50} values were derived from dose response curves generated from duplicate data points. Values with standard deviations (in parentheses) are means of at least three independent experiments.
[b] nd = not determined.

group to afford the 2,5-substituted benzamides provided a 3- to 7-fold improvement in binding activity across the series. The effect was most dramatic in compound **57** (2-NH_2,5-CF_3) where a 7-fold improvement in binding activity and functional activity over **1** was observed. To add evidence that these compounds exerted their effects on THP-1 cells specifically through CCR2, compound **57** was further evaluated in an [^{125}I]-MCP-1 binding assay using HEK293 cells transfected with the hCCR2b receptor. The observed binding IC_{50} of 45 nM was consistent with the binding IC_{50} observed in the THP-1 cell line. The effect of compound **57** on CCR1 was also measured using [^{125}I]-MIP-1α and THP-1 cells showing 25% inhibition at 1 μM (IC_{50} > 1μM), indicating more than 50-fold selectivity over the related chemokine receptor.

Re-optimization of R^1 substitution on the benzyl group in the presence of preferred amino acid spacer glycine and 5-substituted 2-anthranilimides afforded extremely potent CCR2b antagonists. Guided by the SAR developed in earlier compounds disclosed in Table 1, a number of para-substituted benzyl groups were examined with the new anthranilamides. Not unexpectedly, the most active compounds were found to contain the 5-trifluoromethyl-2-anthranilamide for R^2, which are listed in Table 3. A relatively flat SAR was obtained for the incorporation of a single electron-donating substituent in the 4-position at R^1 (Compounds **58**–**64**, binding IC_{50} 11–42 nM). An improvement in activity could be achieved by the incorporation of an additional electron-donating substituent in the 2- or 3- position of the benzyl ring. Several of these 2,4- and 3,4-disubstituted compounds exhibited single-digit nanomolar binding affinity for the CCR2b receptor and potently inhibited MCP-1-induced chemotaxis (Compounds **65**–**72**). Compound **71** was the most active compound in this series and was a potent inhibitor of MCP-1 binding (IC_{50} 3.2 nM) as well as a sub-nanomolar inhibitor of MCP-1 induced chemotaxis (IC_{50} 0.83 nM).

Several compounds were chosen for further evaluation in an additional functional assay: the MCP-1 induced Ca^{2+} flux assay. [18] Inhibition of the release of Ca^{2+} was observed for all compounds tested and a close correlation between the binding IC_{50} and the inhibition of Ca^{2+} release was observed (see Table 4). Compounds incubated with THP-1 cells in the absence of MCP-1 did not elicit a Ca^{2+} flux and therefore were not partial agonists, but antagonists (data not shown).

Table 4. MCP-1-Induced Ca^{2+} flux assay data for selected compounds

Compound	Binding IC_{50}[a] (nM)	Chemotaxis IC_{50}[a] (nM)	Ca^{2+} Flux IC_{50}[b] (nM)
19	116 (31)	12.4 (0.3)	64
25	226	5.5	365
58	26	3.6	23.1
61	11 (6)	0.89	5.3
71	3.2 (2.6)	0.83	7.5

[a] IC_{50} values were derived from dose response curves generated from duplicate data points. Values with standard deviations (in parentheses) are means of at least three independent experiments.

[b] IC_{50} values are averages from dose response curves generated from duplicate data points from two independent experiments.

In conclusion, high-throughput parallel synthesis allowed us to rapidly explore the SAR of all three components (R^1 substituted benzyl group, R^3 amino acid spacer and R^2 substituted benzamide) of the (*R*)-3-amino pyrrolidine series **2** in a systematic fashion. Significant improvements in binding affinity and functional activity were achieved and compound **71** (binding IC_{50} 3.2 nM, chemotaxis IC_{50} 0.83 nM) showed a >60-fold improvement over lead compound **1**. The potent CCR2b antagonists described herein will be useful in the studies on the role of MCP-1 and CCR2 in diseases where monocyte trafficking plays a role.

Acknowledgments

The authors wish to acknowledge Dr. Erin Bradley and Dr. David Spellmeyer for computational support on this program, Dr. Dan Kassel, Dr. Lu Zeng and Ms. Xiaoli Wang for their technical expertise in setting up systems for mass triggered HPLC purification, Ms. Akiko Takeuchi for her expertise on the Ca^{2+} flux inhibition assay and Dr. Takeshi Hara and Dr. Seizi Kurozumi for general support.

References and notes

1. (a) Rollins, B. J. *Blood* **1997**, *90*, 909; (b) Saunders, J.; Tarby, C. M. *Drug Discov. Today* **1999**, *4*, 80; (c) Murphy, P. M.; Baggiolini, M.; Charo, I. F.; Hebert, C. A.; Horuk, R.; Matsushima, K.; Miller, L. H.; Oppenheim, J. J.; Power, C. A. *Pharmacol. Rev.* **2000**, *52*, 145; (d) Horuk, R. *Cytokine Growth Factor Rev.* **2001**, *12*, 313; (e) Carter, P. H. *Curr. Opin. Chem. Biol.* **2002**, *6*, 510; (f) Schwarz, M. K.; Wells, T. N. C. *Nat. Rev. Drug Disc.* **2002**, *1*, 347; (g) Charo, I. F.; Ransohoff, R. M. *N. Eng. J. Med.* **2006**, *354*, 610.
2. (a) Rollins, B. J.; Morrison, E. D.; Stiles, C. D. *Proc. Natl. Acad. Sci. U.S.A.* **1988**, *85*, 3738; (b) Charo, I. F.; Myers, S. J.; Herman, A.; Franci, C.; Connolly, A. J.; Coughlin, S. R. *Proc. Natl. Acad. Sci. U.S.A.* **1994**, *91*, 2752.
3. Boring, L.; Gosling, J.; Chensue, S. W.; Kunkel, S. L.; Farese, R. V., Jr.; Broxmeyer, H. E.; Charo, I. F. *J. Clin. Invest.* **1997**, *100*, 2552.
4. Lu, B.; Rutledge, B. J.; Gu, L.; Fiorillo, J.; Lukacs, N. W.; Kunkel, S. L.; North, R.; Gerard, C.; Rollins, B. J. *J. Exp. Med.* **1998**, *187*, 601.
5. (a) Ogata, H.; Takeya, M.; Yoshimura, T.; Takagi, K.; Takahashi, K. *J. Pathol.* **1997**, *182*, 106; (b) Gong, J.-H.; Ratkay, L. G.; Waterfield, J. D.; Clark-Lewis, I. *J. Exp. Med.* **1997**, *186*, 131.
6. (a) Boring, L.; Gosling, J.; Cleary, M.; Charo, I. F. *Nature* **1998**, *394*, 894; (b) Dawson, T. C.; Kuziel, W. A.; Osahar, T. A.; Maeda, N. *Atherosclerosis* **1999**, *143*, 205.
7. Lloyd, C. M.; Minto, A. W.; Dorf, M. E.; Proudfoot, A.; Wells, T. N. C.; Salant, D. J.; Gutierrez-Ramos, J.-C. *J. Exp. Med.* **1997**, *185*, 1371.
8. Kennedy, K. J.; Strieter, R. M.; Kunkel, S. L.; Lukacs, N. W.; Karpus, W. J. *J. Neuroimmunol.* **1998**, *92*, 98.
9. For reviews see: (a) Carter, P. H.; Cherney, R. J.; Mangion, I. K. In *Ann. Rep. Med. Chem*; Macor, J. E., Ed.; Academic Press: London, 2007; vol. 42, pp 211–227; (b) Trivedi, B. K.; Low, J. E.; Carson, K.; LaRosa, G. J.. In *Ann. Rep. Med. Chem*; Doherty, A. M., Ed.; Academic

Press: London, 2000; pp 191–200; (c) Feria, M.; Diaz-Gonzalez, F. *Exp. Opin. Ther. Patents* **2006**, *16*, 49; (d) Dawson, J.; Miltz, W.; Mir, A. K.; Wiessner, C. *Exp. Opin. Ther. Targets* **2003**, *7*, 35.

10. (a) Imai, M.; Shiota, T.; Kataoka, K.; Tarby, C. M.; Moree, W. J.; Tsutsumi, T.; Sudo, M.; Ramirez-Weinhouse, M. M.; Comer, D.; Sun, C.-M.; Yamagami, S.; Tanaka, H.; Morita, T.; Hada, T.; Greene, J.; Barnum, D.; Saunders, J.; Myers, P. L.; Kato, Y.; Endo, N. *Bioorg. Med. Chem. Lett.* **2004**, *14*, 5407; (b) Moree, W. J.; Kataoka, K.; Ramirez-Weinhouse, M. M.; Shiota, T.; Imai, M.; Sudo, M.; Tsutsumi, T.; Endo, N.; Muroga, Y.; Hada, T.; Tanaka, H.; Morita, T.; Greene, J.; Barnum, D.; Saunders, J.; Myers, Y.; Kato, P. L.; Tarby, C. M. *Bioorg. Med. Chem. Lett.* **2004**, *14*, 5413.
11. Fivush, A. M.; Wilson, T. M. *Tetrahedron Lett.* **1997**, *38*, 7151.
12. (a) Zeng, L.; Kassel, D. B. *Anal. Chem.* **1998**, *70*, 4380; (b) Zeng, L.; Wang, X.; Wang, T.; Kassel, D. B. *Comb. Chem. High-Throughput Screen.* **1998**, *1*, 101.
13. For a description of the binding assay see Ref. 10a.
14. Falk, W.; Goodwin, R. H., Jr.; Leonard, E. J. *J. Immunol. Methods* **1980**, *33*, 239.
15. Topliss, J. G. *J. Med. Chem.* **1977**, *20*, 463.
16. For example, replacement of Gly in compound **1** with D/L-Ala resulted in a MCP-1 binding IC_{50} of 22 μM, replacement with β-Ala gave an IC_{50} of 10 μM.
17. (a) Craig, P. N. *J. Med. Chem.* **1972**, *15*, 144; (b) Craig, P. N. *J. Med. Chem.* **1971**, *14*, 680.
18. Typical procedure for the Ca^{2+} flux assay: THP-1 cells were cultured in HBSS loading buffer supplemented with 1% fetal bovine serum (FBS) and 20 mM HEPES. After centrifugation, cells were loaded for 30 min with the Ca^{2+} sensitive fluorescent dye Fluo-3 AM (2 million cells/mL in RPMI medium containing 4 μM Fluo-3 AM, 20 mM HEPES, 0.1% bovine serum albumin (BSA), and 5 mM probenecid). Excess dye was removed by 3-fold washing with buffer (5 mM HEPES, 140 mM NaCl, 1 mM $MgCl_2$, 5 mM KCl, 10 mM glucose, 2.5 mM probenecid, 1.25 mM $CaCl_2$, and 0.1% BSA; all further incubations were done in this matter). Cells were plated at a density of 150,000 cells/well in dark-wall 96-well plates and sedimented by centrifugation (1 min). The cells were pre-incubated for 3 min with test compound. Then 10^{-7} M human MCP-1 was added. Changes in intracellular free Ca^{2+} concentration were measured using the Fluorescent Imaging Plate Reader (FLIPR). Fluorescence was recorded in two consecutive sequences. Each sequence was comprised of 60 s (recordings at 1 s intervals) followed by 120 s (recordings at 6 s intervals). Test compound was added at 10 s into the first sequence. MCP-1 was added at 10 s into the second sequence. After addition in each sequence, further analysis was made for 50 s (recordings at 1 s intervals) and 120 s (recordings at 6 s intervals).